ACS APPLIED MATERIALS & INTERFACES

RESEARCH ARTICLE

www.acsami.org

Localized In situ Polymerization on Graphene Surfaces for Stabilized Graphene Dispersions

Sriya Das, Ahmed S. Wajid, John L. Shelburne, Yen-Chih Liao, and Micah J. Green*

Department of Chemical Engineering, Texas Tech University, Lubbock, Texas 79409, United States

Supporting Information

ABSTRACT: We demonstrate a novel in situ polymerization technique to develop localized polymer coatings on the surface of dispersed pristine graphene sheets. Graphene sheets show great promise as strong, conductive fillers in polymer nanocomposites; however, difficulties in dispersion quality and interfacial strength between filler and matrix have been a persistent problem for graphene-based nanocomposites, particularly for pristine graphene. With this in mind, a physisorbed polymer layer is used to stabilize graphene sheets in solution. To create this protective layer, we formed an organic microenvironment around dispersed graphene sheets in surfactant solutions, and created a nylon 6, 10 or nylon 6, 6 coating via interfacial polymerization. Technique lies at the intersection of emulsion and admicellar polymerization; a similar technique was originally developed to protect luminescent properties of carbon nanotubes in solution. These coated graphene dispersions are aggregation-resistant and may be reversibly redispersed in water even after freeze-drying. The coated graphene holds promise for a number of applications, including multifunctional graphene−polymer nanocomposites.

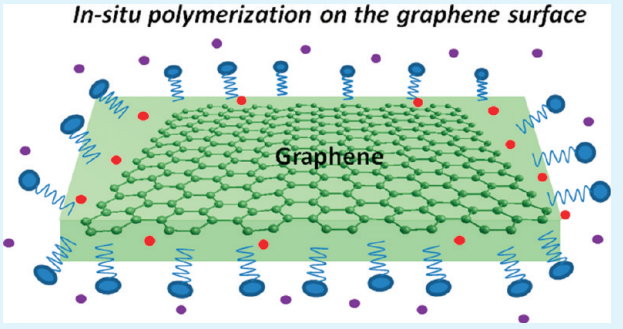

KEYWORDS: graphene, nanocomposite, nylon, polymer, in situ polymerization, admicellar polymerization

Single-layer graphite, known as graphene, has attracted considerable scientific interest in recent years because graphene's unique mechanical, electrical, and thermal properties may enable a range of advanced materials and devices including nanocomposites[1−5] and thin conductive films.[6,7] Graphene is a two-dimensional structure of sp^2-hybridized carbon atoms arranged in a honeycomb lattice.[8] Graphene was originally isolated through micromechanical cleavage of graphite; this discovery was recently honored with the 2010 Nobel Prize in Physics.[9] However, this method is limited because of the lack of scalability. Recent advancements in the production of graphene involve chemical vapor deposition,[10] epitaxial growth, and liquid phase exfoliation from graphite. This latter method is best suited to the scalable production of multifunctional advanced materials (such as composites) based on graphene.

However, dispersion of graphene in common solvents is challenging because exfoliation from graphite is hindered by the strong, attractive van der Waals forces holding the sheets together. Even after the initial process of exfoliation and dispersion, those same attractive forces cause graphene to reaggregate. We briefly review the common techniques used to address this issue.

The most common technique for exfoliation and dispersion of graphene is the oxidation of graphite to form graphite oxide.[11−13] The graphite oxide is hydrophilic and is easily exfoliated in water and other solvents as single sheets, termed graphene oxide (GO). The presence of the carboxyl and epoxide groups on the basal plane of GO reduce the interlayer forces and render them soluble in water. (Note that recent work has suggested that GO is not actually soluble in water and other solvents; instead, oxidative debris acts as a stabilizer.[14]) GO may be reduced using hydrazine in the presence of stabilizers such as surfactants or polymers to yield chemically converted graphene (CCG).[11] The stabilizers wrap around the graphene and sterically prevent reaggregation.[12,13] Additional functional groups may be bonded to GO or CCG to increase solubility in a range of solvents.[15−18] However, this approach suffers from certain drawbacks. The reduction of GO to CCG is incomplete such that some of the sp^3 characteristics of GO are still retained in the CCG.[11] This process only partially restores the unique properties of pristine graphene; in fact, the electrical conductivity of CCG is 2 orders of magnitude lower than pristine graphene.[19]

Alternatively, liquid phase exfoliation of graphene as few-layer sheets may be obtained in certain organic solvents without chemical modification.[6,20] The use of organic solvents such as NMP yields defect-free monolayer graphene dispersions,[21] but the concentrations of the dispersions are comparatively low (<0.01 mg/mL) and require extensive sonication. Chlorosulfonic acid acts as an excellent solvent for graphene and yields graphene dispersions with concentrations as high as 2 mg/mL; unfortunately, such superacids are incompatible with most composite applications.[22] Intercalation compounds such as potassium intercalants are used to increase the distance in between the consecutive layers of graphite; these

Received: November 20, 2010
Accepted: May 3, 2011
Published: May 03, 2011

intercalation compounds aids in the exfoliation of graphene without functionalization or sonication.[23,24]

Aqueous dispersions of pristine graphene may be prepared by sonicating graphite in the presence of stabilizers; such stabilizers include polymers, such as poly vinyl pyrrolidone (PVP), or surfactants, such as sodium chlorate and sodium dodecyl benzene sulfonate (SDBS).[25−32] The surfactant technique yields high concentration dispersions of graphene (>0.3 mg/mL).[31]

For composite applications, excellent dispersion is not enough; one must also have excellent interfacial adhesion for efficient stress transfer from the graphene to the polymer matrix. These two issues of poor dispersion and poor interfacial strength between filler and matrix is a persistent problem for composites with pristine nanomaterial fillers.[33] Composites of graphene nanoribbons (GNR)[34] and graphene platelet[35,36] with an epoxy matrix have shown a considerable increase in mechanical properties; however, the graphene platelets used in these composites are either GO or CCG since dispersion of pristine graphene is challenging. Furthermore, surfactant-free graphene is desirable since presence of surfactant may affect the transparency, thermal properties, and mechanical properties of the composite.[37−40] The ability to form polymer coatings on pristine graphene surfaces may address this issue of interfacial strength.

In the present work, we aim to address these needs; we utilize an in situ polymerization technique to encapsulate the graphene sheets with a polymer coating. Our work lies at the intersection of emulsion polymerization (where polymerization occurs at the organic-aqueous interface inside micelles in the bulk solution) and admicellar polymerization (where polymerization occurs at a surface coated by a surfactant bilayer). Admicellar polymerization refers to the process in which a thin film of polymer is deposited on a solid surface. This polymerization process is observed to go through three major steps: (1) the aggregation of surfactants at solid−liquid interfaces to form bilayer (admicelles) through adsorption from an aqueous solution (2) introduction of the hydrophobic monomer which travels to the inner-core of the surfactant (monomer adsolubilization) and (3) initiation of the polymerization by mechanisms similar to those occurring in emulsion techniques. In case of the admicellar polymerization, the surfactant concentration is maintained to be always below the critical micelle concentration (cmc) to avoid polymerization in the bulk solution. This technique was used to coat various substrates with polymers like polystyrene (PS) and poly methyl methacrylate (PMMA).[41−45] This coating technique was also applied to study the method of polymer coating formation on graphite and mica surfaces.[46−50] Chen et al. had previously demonstrated that the micelle surrounding single-walled carbon nanotubes (SWNTs) could be swelled by various organic solvents.[51] They then developed a technique to coat surfactant-stabilized SWNTs with nylon 6,10 by interfacial polymerization within the micelle to preserve SWNT optical properties in solution.[52] We hypothesized that such a technique could be retrofitted to graphene dispersions despite the substantial differences in surfactant structure between stabilized SWNTs and graphene. This work is a combination of both emulsion and admicellar polymerization, as the graphene is inside the micelle and a thin polymer coating is deposited on the graphene surface. Whereas Chen et al. focused on SWNT optical properties, our ultimate application is graphene-based composites. The polymer-coating should blend well with the polymer matrix and facilitate stress transfer and transport of properties in the composite; this issue of load transfer is one of the more pressing problems in the field of nanocomposites.

We first swell the surfactant micelle around the graphene with organic solvents, and polymerization performed at the interface between water and organic solvents creates a nylon 6,10 coating on the graphene surface. (This technique can be used to create nylon 6,6 coatings as well.) The coated graphene can be freeze-dried and redispersed effectively in water. The coating aids the redispersion of graphene in water without any visible aggregation by forming a polymer layer around the graphene and preventing van der Waals induced aggregation. We characterize our dispersions through a variety of techniques, including rheology, absorbance, AFM, TEM and SEM imaging. The polymer-coated graphene holds great promise as a means to increase the interfacial strength in polymer nanocomposites.

EXPERIMENTAL PROCEDURE

Stable dispersions of graphene in water are prepared with sodium dodecyl benzene sulfonate (SDBS) (MPBiochemicals, # 157889) as the surfactant. Expanded graphite (1.29 g), (Asbury Carbons, CAS# 7782−42−5, grade 3805) is added to a 15 mL (2%w/v) solution of SDBS (The use of graphite flakes instead of expanded graphite yields similar results). The use of 2% w/v ratio (20 mg/mL) of surfactant is adopted from the work of Green et al., where sodium cholate is used to stabilize graphene in water.[29] The critical micelle concentration of SDBS is usually found to be 2.9 mM (1 mg/mL) at 298 K.[53] This solution is tip sonicated using a Misonix sonicator (XL 2000) at output wattage of 7 W for 1 h. The sample is further centrifuged (Centrific Centrifuge 225, Fischer Scientific) overnight (12 h) at a speed of ∼5000 rpm to remove larger aggregates, and the supernatant is collected.

A 0.5 M sebacoyl chloride (Sigma Aldrich, 99%) solution in carbon tetrachloride (Acros Organics, 99%) is used to swell the micelle structure over the graphene. (To make nylon 6,6 rather than nylon 6,10, we used adipoyl chloride rather than sebacoyl chloride.) The surfactant/graphene dispersion is carefully added to the organic solution in a 1:1 ratio, shaken and allowed to stand for one hour for phase separation. The organic solvent forms an interface and swells the micelle interior. After phase separation, the swelled aqueous surfactant/graphene dispersion is separated from the suspension. Hexamethylene diamine (Sigma Aldrich, 98%) is melted at 50 °C and 2 μL is added to the swelled aqueous dispersion dropwise using a micropipet. Hexamethylene diamine and sebacoyl chloride react at the water/organic interface to form nylon on the surface of the graphene.

To measure the concentration of the dispersions, we filtered the samples through Teflon filters (Millipore, 0.2 μm), dried them overnight at 40 °C, and carefully measured the change in mass of the filter paper. On the basis of prior TGA analysis,[30] we estimate that ∼64% of the residue on the filter paper is graphitic. (The same filter papers are also used to measure Raman spectra on a Renishaw Raman microscope using a 633 nm He−Ne laser.) To correlate concentration with absorbance, we performed UV−vis spectroscopy on a Shimadzu UV−vis spectrophotometer 2550 at wavelengths of 200−800 nm. To eliminate the background effect, i.e., the effects of surfactant spectrum, we measured the absorbance against the surfactant solution.

As a check for dispersion stability at low pH, the pH of the surfactant-stabilized graphene dispersion is lowered by adding 1.2 M HCl solution to it and centrifuging the sample at ∼5000 rpm for 1 h; this is directly compared against the low-pH nylon-coated graphene dispersion.

As an additional check for stability against van der Waals aggregation, both the surfactant-stabilized graphene and the nylon-coated graphene dispersions may be freeze-dried (Vitris Benchtop Freeze-Dryer) overnight to yield dry samples. The freeze-dried samples are redispersed in water without any sonication for rheological and other analysis. Rheological

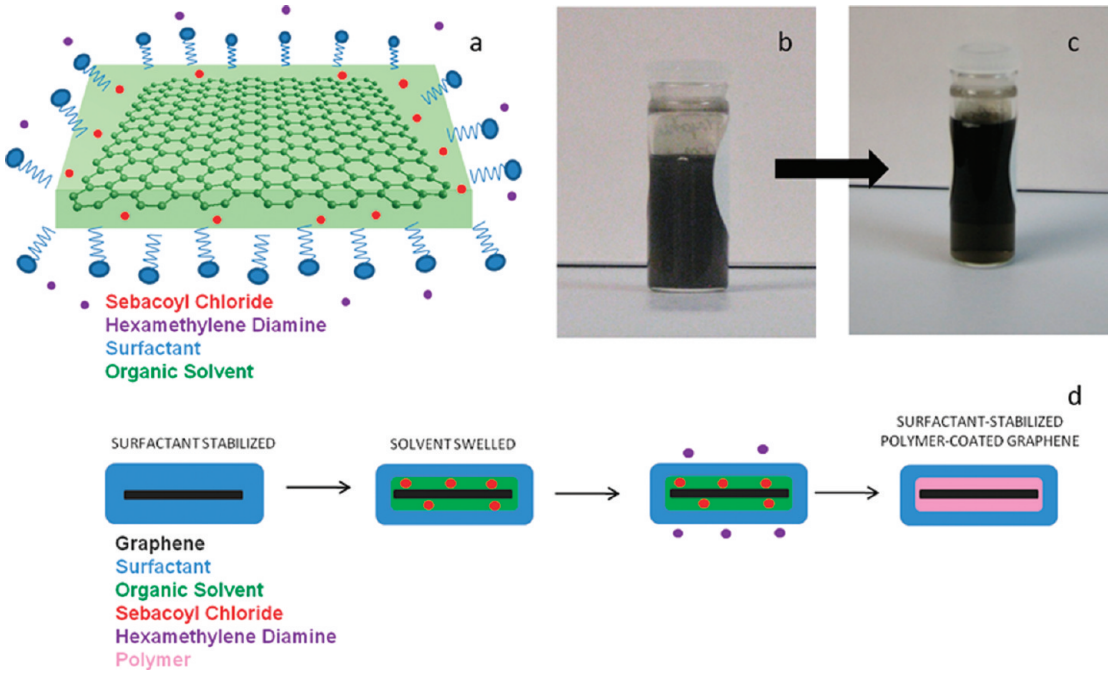

Figure 1. (a) Schematic representation of mechanism of wrapping of nylon around graphene. Photographs of (b) aqueous dispersion of surfactant-stabilized graphene and (c) aqueous dispersion of nylon-coated surfactant-stabilized graphene. (d) Schematic representation of the polymerization technique to stabilize graphene.

experiments are done using a double Couette fixture (C-DG26.7/T200/SS) on a shear rheometer (Anton Paar, USA). To prevent the evaporation of the samples, a solvent trap is used. The shear-viscosity behavior of aqueous samples was measured before freeze-drying and after freeze-drying and redispersion.

The structure of the graphite flakes and the nylon-coated graphene is characterized by FT-IR spectroscopy (Nexus 470).For FTIR analysis, ethyl acetate (EA) (5 mL) is added to the nylon-coated samples and further freeze-dried (EA removes the surfactant from the system). After phase separation, the nylon/graphene portion is carefully removed from the EA portion.

Tapping mode AFM analysis is done on a Veeco Multimode AFM (IIIa) with NSC14 cantilevers (MikroMasch). AFM samples are prepared by spin coating ~20 μL of the dispersion onto a freshly cleaved mica surface at 3000 rpm for 20 s. The spin-coated mica is further dried on a hot plate at 50 °C for 1 min.

TEM samples are prepared by drop coating the sample on holey carbon grids and air-dried for 1 min. A voltage of 100 keV is used to image the specimens on a Hitachi H8100.

SEM samples are prepared by mounting the samples on double-faced carbon tape and sputter coating with gold at 10 mA current for 1 min. A voltage of 2 keV is used to image the specimens on a Hitachi S4300 SE/N.

RESULTS AND DISCUSSIONS

The schematic representation (Figure 1a) shows the basic mechanism of polymerization and coating around the graphene. First, the graphite flakes are sonicated in an SDBS solution. (The ability of SDBS to stabilize graphene dispersions is well-established.[30]) The sonicated sample is then centrifuged to yield a dark solution with no precipitate (Figure 1b). Similar to the SWNT-nylon technique, the surfactant environment is swelled with organic solvent.[52] Carbon tetrachloride (with dispersed sebacoyl chloride) is added to the surfactant-stabilized graphene dispersion, which penetrates into the gap between the surfactant and graphene. This creates a water−organic interface between the graphene surface and the surfactant which is ideal for interfacial polymerization since the monomers for nylon formation are selectively soluble in the water (hexamethylene diamine) and the organic phase (sebacoyl chloride). The hexamethylene diamine is added to the aqueous phase and reacts with sebacoyl chloride at the interface. This creates a thin nylon coating on the graphene pictured in Figure 1c. The stepwise mechanism of the emulsion polymerization is demonstrated in Figure 1d. In the case of admicellar polymerization, the organic monomer is typically added to the aqueous phase. In our work, we use an organic solvent to aid the transportation of the organic monomer to the hydrophobic core of the surfactant micelles.

We utilize a range of characterization techniques to establish that (1) we begin with a high-concentration surfactant-stabilized few-layer graphene dispersion, (2) the nylon polymerization is successful and the dispersion remains stable, and (3) the nylon protects the graphene from van der Waals aggregation in scenarios (low pH, freeze-drying) where simple surfactant stabilization would not. This final point is especially critical because the creation of aggregation-resistant graphene opens up a wide range of novel applications for graphene, particularly in the field of composite melt-mixing.

The concentrations of the centrifuged phase of the graphene dispersions are determined by vacuum filtration. In the case of the SDBS/graphene dispersions, the concentration is found to be 0.2 mg/mL (comparable to 0.09−0.3 mg/mL for sodium cholate[29,31] and 0.05 mg/mL for SDBS[30]). These concentrations are quantitatively correlated with the absorbance spectra. According to Lambert−Beer's law, the absorption coefficient of any substance varies linearly with the concentration. The absorbance spectra of the dispersions of surfactant-stabilized graphene, solvent-swelled surfactant stabilized graphene and surfactant-stabilized nylon-coated-graphene are provided in the Supporting

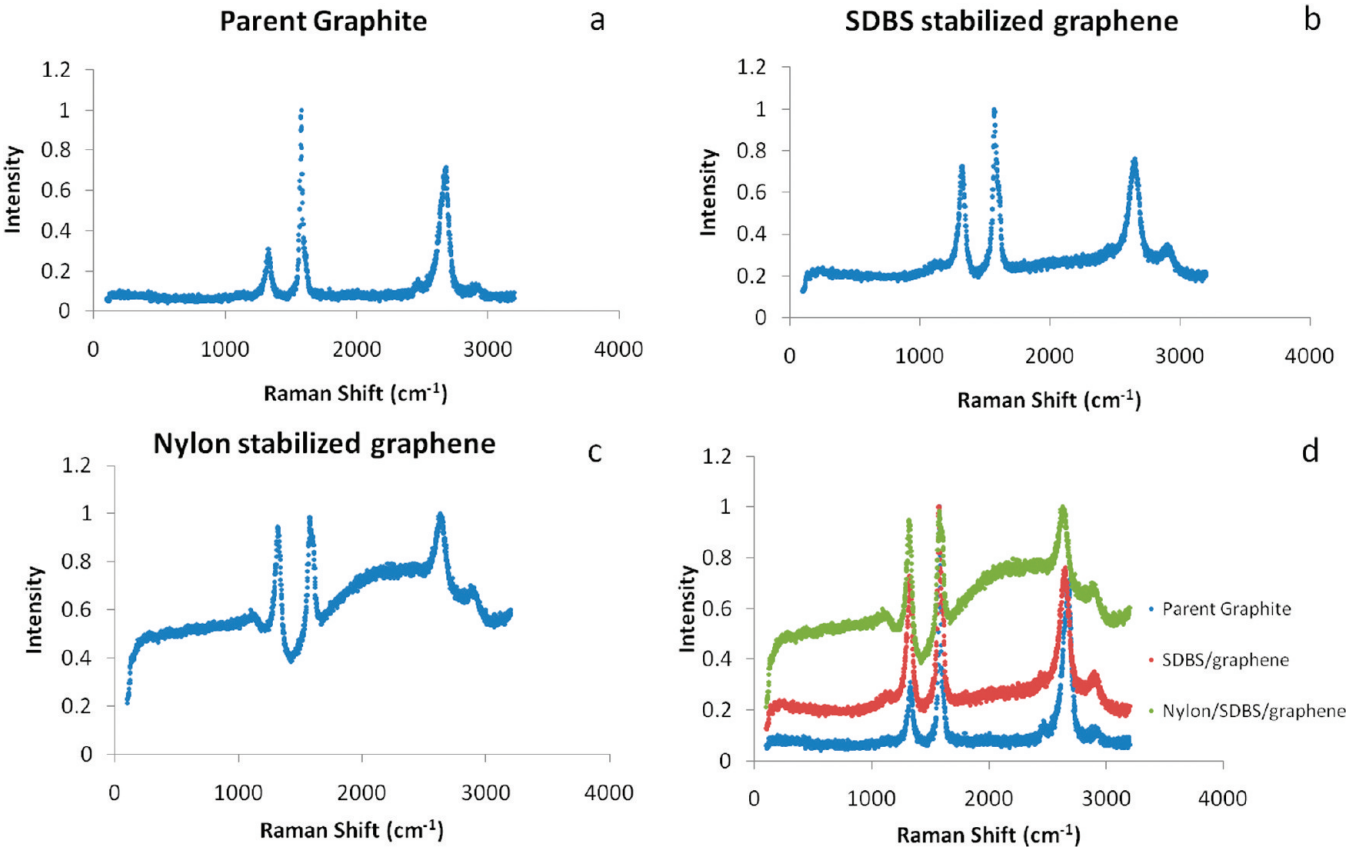

Figure 2. Raman spectra of (a) parent graphite (expanded graphite) (EG), (b) SDBS/graphene, (c) nylon/SDBS/graphene, and (d) the comparison of all the spectra. In the spectra of surfactant-stabilized and polymer-coated graphene, we observe an increase in the intensity of the D-peak. As the graphene flake size decreases, the number of edges of the graphene exposed per flake increases. The sp^3 characteristic of the edges contributes to the intensity of the D-peak. The exfoliation of SDBS/graphene and the polymer-coated graphene is confirmed by a G-peak shift (~3 cm^{-1}).

Information (Figure S1). Figure S2 in the Supporting Information shows the optical absorbance as a function of different concentrations of the graphene dispersions. We determined the extinction coefficient (α) at a wavelength of 660 nm using the linear relationship between the absorbance and calculated concentration for a particular dispersion ($A = \alpha lC$; where l is the cell length). Absorbance at 660 nm wavelength was used by Lotya et al. to calculate the extinction coefficients for the same system.[30,54] In case of our SDBS/graphene dispersion, α is found to be 1660 mL mg^{-1} m^{-1}, which is in reasonable agreement with the values of extinction coefficient values (1390 mL mg^{-1} m^{-1}) obtained by Lotya et al.[30]

The degree of exfoliation is measured by Raman spectroscopy. The parent expanded graphite (Figure 2a) shows a very sharp G peak and comparatively smaller 2D peak at 2700 cm^{-1}. In the spectra of surfactant-stabilized (Figure 2b) and polymer-coated graphene (Figure 2c) the intensity of the D-peak increases. Prior studies have shown that as the graphene flake size decreases, the number of graphene edges exposed per flake increases.[21,22,29,32,55,22,55] These edges have sp^3 characteristics which contribute to the increases in D-peak intensity. The 2D peak position for graphene is 3−5 cm^{-1} shifted relative to the parent graphite.[55] The SDBS/graphene and the polymer-coated graphene show a G-peak shift (~3 cm^{-1}), which indicates exfoliation of graphene. The 2D peak ideally should be around four times as intense as the G-peak for monolayer graphene.[55] In Figure 2c, the intensity of the 2D peak has a larger intensity compared to the G peak, which depict that the coated graphene is a few layers thick. Figure 2d shows a comparison of all the three

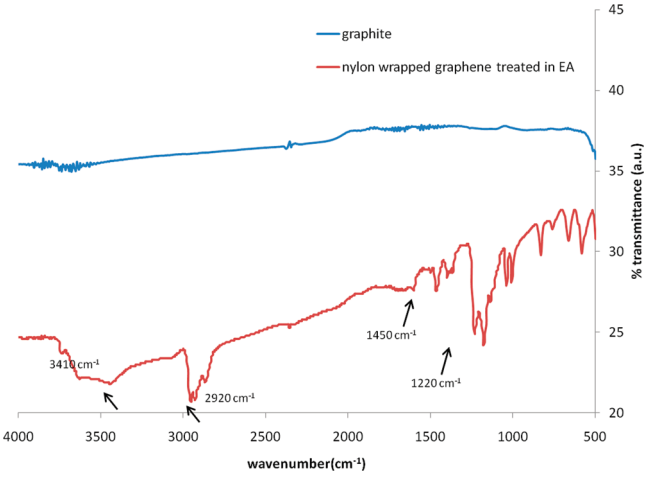

Figure 3. FTIR spectra of raw and nylon/graphene. The effect of the surfactant is removed by treating the coated graphene with ethyl acetate (EA). The distinct peaks of C−H stretching at 1220 and 2920 cm^{-1}, the amide-II peaks at 1450 cm^{-1}, and a broad peak of the N−H stretching at 3410 cm^{-1} in case of the polymer-coated graphene confirms the nylon formation.

dx.doi.org/10.1021/am1011436 |ACS Appl. Mater. Interfaces 2011, 3, 1844–1851

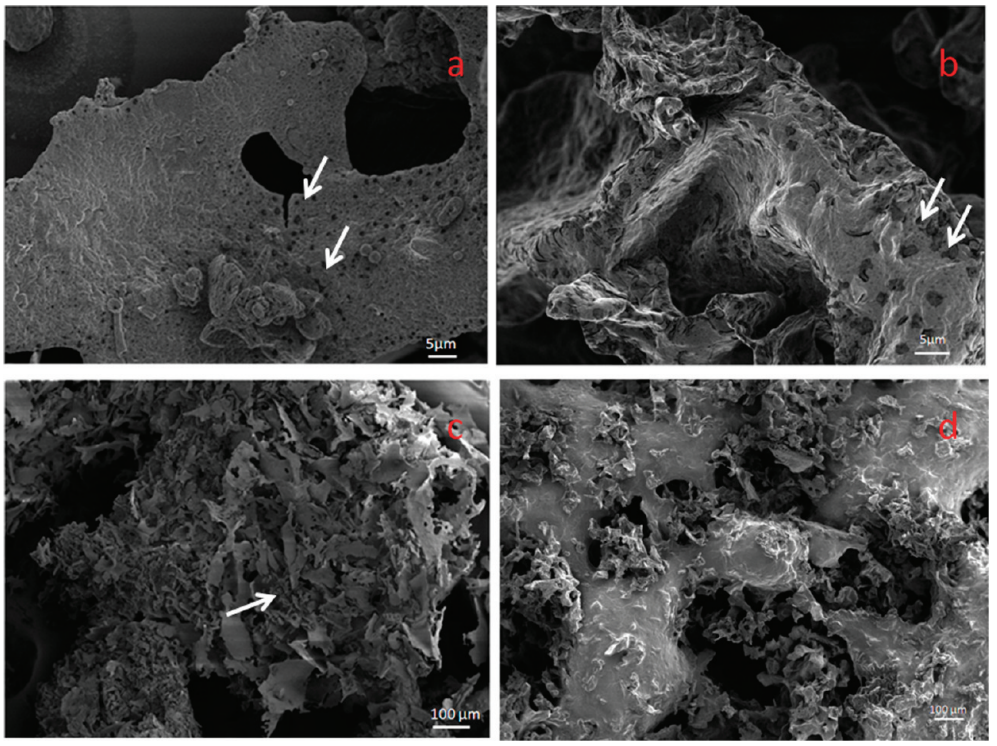

Figure 4. SEM images on freeze-dried samples of (a) SDBS/graphene, (b) nylon/SDBS/graphene; magnified views of freeze-dried samples of (c) SDBS/graphene, (d) nylon/SDBS/graphene. The surfactant-stabilized and nylon-coated surfactant-stabilized graphene samples show no visible aggregation under the EM studies.

samples tested. These observations confirm the exfoliation of few-layer graphene.

FT-IR spectroscopy is performed on the freeze-dried samples of surfactant-stripped, nylon-coated graphene and parent graphite flakes to investigate the chemical change caused by the polymerization.[52] Similar to the nylon-coated SWNTs, the nylon-coated graphene also exhibits characteristic amide-I, amide-II, N−H and C−H stretches in the FT-IR spectrum. Figure 3 shows spectral comparison where the transmittance of graphite is shifted by a constant, for clarity. The polymer-coated graphene sample shows distinct peaks of C−H stretching at 1220 cm^{-1} and 2920 cm^{-1}, the amide-II peaks at 1450 cm^{-1}, and a broad peak of the N−H stretching at 3410 cm^{-1}. A comparison between the spectra of graphite flakes and polymer-coated graphene confirms that nylon formation occurs in the bulk solution similar to Chen et al.

Figure 4 shows SEM images of the freeze-dried samples. The surfactant-stabilized sample and nylon-coated graphene sample exhibit a strong morphological difference. The coated sample (Figure 4b) can be identified by the difference of the appearance in the image. The magnified views of the freeze-dried samples are shown in Figure 4c,d. More SEM images of the vacuum-filtered films and ethyl acetate treated vacuum-filtered films of the surfactant-stabilized sample and nylon-coated graphene are provided in the Supporting Information (Figure S3).

To access the number of layers of the graphene in the dispersions, we performed tapping mode AFM analysis on the samples. An AFM image of surfactant-stabilized graphene is shown in Figure 5a. Prior work has shown that the graphene in the surfactant-stabilized aqueous graphene dispersions is indeed single-to-few layers thick.[29,30] In our images, we also observe that the surfactant stabilizes single-to-few layer graphene. The height ranges from 1 to 2.5 nm. The surfactant is deposited on the graphene in an irregular fashion. The layer of surfactant is found to have a patchy appearance. The presence of the surfactant on single-to-few layer graphene accounts for the variation in thickness. Figure 5b shows the graphene flakes after interfacial polymerization. The thickness variation in this case is 4−6 nm. The polymerization changes the morphology of the surface without causing aggregation. The thin coating of nylon on the graphene causes the increase in thickness. Prior work has shown that the polymer usually gets deposited on the substrate in the form of "patches" or islands. AFM measurements on mica and graphite surfaces reveal that the polymer film formation is indeed discontinuous.[46,50,56,57] In the case of the AFM images of our polymer-stabilized graphene, we observe an irregular deposition of the polymer on the graphene surface. The AFM images of irregular polymer deposition are similar to those of See et al. and Marquez et al.,[49,57] who observed polymerization on graphite surfaces. For completeness, more results on the AFM performed on the nylon-coated surfactant-stabilized graphene are provided in the Supporting Information (Figure S4). The nylon-coated graphene can be easily redispersed after freeze-drying, and to check the dispersion quality, we take AFM images after redispersion (Figure 5c). There is no change in thickness of the graphene flakes after redispersion. This gives an evidence of an excellent redispersion of coated-graphene in water without aggregation. We revisit this issue below by making rheological measurements.

We also use TEM to confirm the presence of single-to-few layer stabilized graphene in our dispersions. A TEM image of the nylon-coated graphene is shown in Figure 6a. The edge of a graphene sheet can reveal the number of layers present. Figure 6b

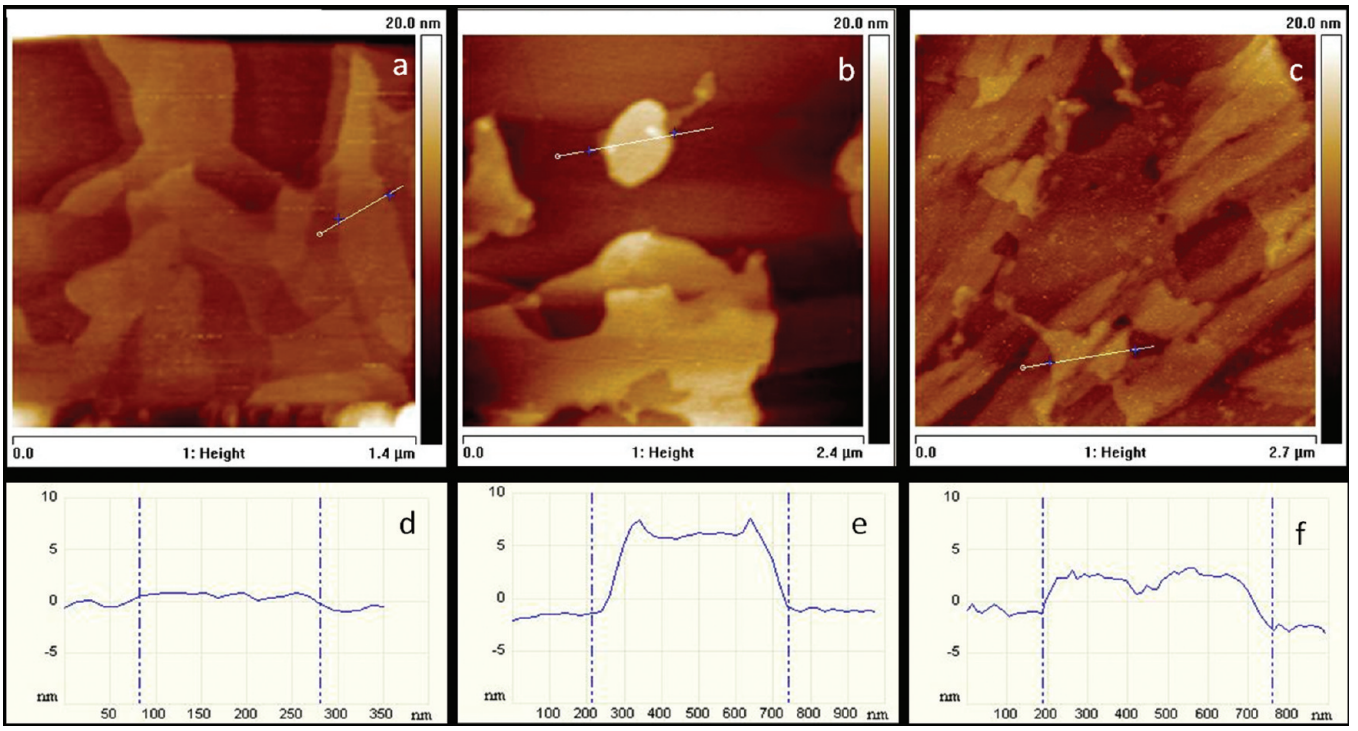

Figure 5. AFM of the (a) SDBS/graphene, (b) nylon/SDBS/graphene, (c) redispersed nylon/SDBS/graphene, (d) height profile of the flake in SDBS/graphene, (e) height profile of the flake in nylon/SDBS/graphene, (f) height profile of the flake in redispersed nylon-coated SDBS-stabilized graphene. In the case of the surfactant-stabilized graphene, the height ranges from 1 to 4 nm, indicating that the graphene is indeed single-to-few layer thick. The nylon-coated graphene shows a height variation of 4−6 nm. The thin coating of nylon on the surfactant-stabilized graphene surface increases the thickness without aggregation. AFM images of the nylon-coated graphene after freeze-drying and redispersion shows no change in thickness of the graphene. This implies excellent redispersion of the coated graphene after freeze-drying.

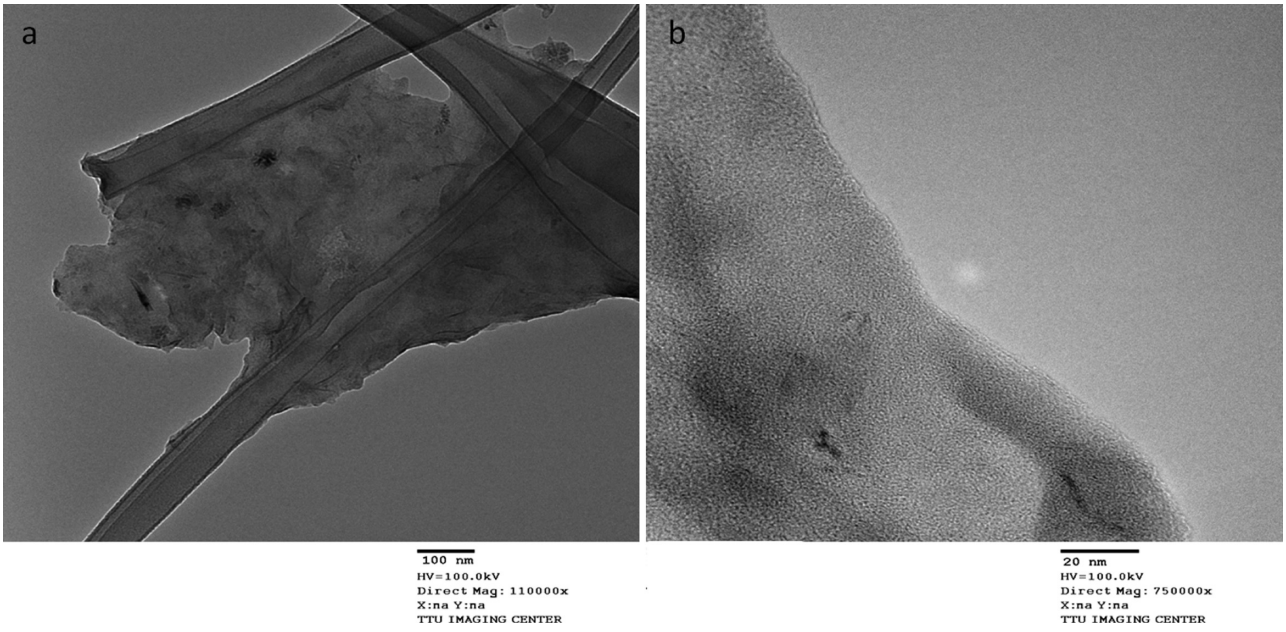

Figure 6. TEM images of (a) nylon/SDBS/graphene; magnified views of (b) nylon/SDBS/graphene. The magnified view of the edges indicates that the graphene is 2−3 layers thick.

shows the SDBS/nylon/graphene dispersion, and the 2−3 layered edges indicate that the graphene is 2−3 layers thick. This is similar to our AFM results on the SDBS/nylon/graphene. Additional TEM images of both SDBS/nylon/graphene and SDBS/graphene are available in the Supporting Information (Figure S5).

As we investigate the differences in dispersion stability caused by the polymerization, we note that the interfacial polymerization

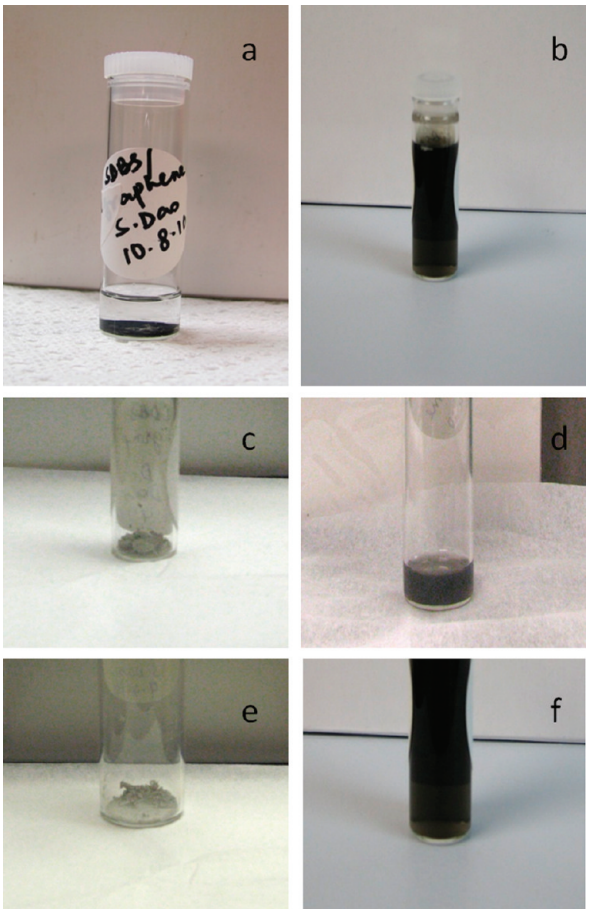

Figure 7. Digital camera images of SDBS/graphene (a) freeze-dried; (b) redispersed in water; nylon/SDBS/graphene (c) freeze-dried; (d) redispersed in water; (e) SDBS/Graphene dispersion at a pH of 2.5; (f) nylon/SDBS/graphene at a pH of 2.5. The interfacial polymerization reaction generates an acidic pH. The pH of the nylon-coated surfactant-stabilized graphene lies in the range of 1.7−2.5. The pH of the SDBS/graphene dispersion is lowered to the same range as the nylon-coated graphene dispersion by adding HCl for the sake of comparison. The SDBS/graphene dispersion destabilizes easily (e), proving that the polymer stabilizes graphene even at the low pH (f).

reaction generates an acidic pH.[52] The measured pH of the nylon-coated surfactant-stabilized graphene is found to be in the range of 1.7−2.5. Prior work showed graphene-PAM dispersions were stable with no aggregation down to a pH of 4.[58] If the pH of our SDBS/graphene dispersions is lowered to the same range as the nylon-coated graphene dispersions, the SDBS/graphene dispersion destabilizes very easily (Figure 7a), whereas the nylon/graphene dispersion remains stable (Figure 7b); this proves that the polymer actually stabilizes graphene at the low pH, similar to the nanotubes results of Chen et al.[52] The coated graphene can thus be processed into graphene-based materials and devices at varying pH conditions.

Additionally, the surfactant stabilized sample (Figure 7c,d) and the nylon-coated sample (Figure 7e,f) can be freeze-dried and redispersed in water without any sonication. Although both the redispersed samples look alike to the eye, we wish to quantify any differences in dispersion quality. Note that in the case of SWNTs, a well-resolved fluorescence spectrum with strong peaks proves that the SWNTs remain as individuals;[52,59] thus, the fluorescence spectra of SWNTs, combined with the absorbance and Raman spectra, give a measure of the dispersion quality. Such a technique is not feasible for graphene because of the absence of fluorescence; instead, we rely on rheological measurements to characterize the dispersion quality before freeze-drying and after redispersion (see Figure S6 in the Supporting Information).

These results may have implications for the processing of graphene-based nanocomposites. In most prior studies, melt mixing of pristine graphene into a polymer matrix has met little success because of difficulties in exfoliation and stable dispersion. Even if the graphene is well-dispersed in the polymer matrix, there still tends to be poor interfacial strength between graphene and polymer matrix, i.e., the load transfer is poor from the matrix to the high-strength filler. For our system, if the nylon-coating treatment were applied to graphene, this coated graphene could easily be melt mixed into a bulk nylon matrix since the coating prevents van der Waals contact between graphene sheets; furthermore, the physisorbed nylon coating should enhance load transfer between the graphene and the surrounding nylon matrix. Preliminary data on such nylon composites loaded with nylon-coated graphene composites are included in the Supporting Information (Figure S7). We aim to explore these issues in future studies.

In summary, we have developed a simple and scalable method to exfoliate graphene in water. In contrast to GO-based methods, no oxidation and reduction are involved in our procedure. We successfully coat the graphene noncovalently with nylon 6,10 and nylon 6,6, and the stability of the graphene dispersion in water is enhanced.

■ ASSOCIATED CONTENT

Ⓢ Supporting Information. More information about absorbance spectra, AFM, HRTEM, rheology, and composites. This material is available free of charge via the Internet at http://pubs.acs.org/.

■ AUTHOR INFORMATION

Corresponding Author
*E-mail: micah.green@ttu.edu.

■ ACKNOWLEDGMENT

We acknowledge Colin Young and Professor Matteo Pasquali of Rice University for their help with the Raman measurements. We acknowledge Wei Zheng and Professor Sindee Simon of TTU for assisting in the FT-IR spectra measurements. We acknowledge Gina Paroline of Anton Paar for her unique insight and help with the rheological measurements. The SEM was performed at the TTU Imaging Center funded by (NSF MRI 04-511) supported by Dr Mark J. Grimson and Professor Lauren S. Gollahon. We thank Professor Brandon Weeks of TTU for his expertise and equipment used in the AFM experiments. We thank Dr. Huipeng Chen and Professor Ronald Hedden of TTU for their helpful insights on nylon composites. Funding was provided by National Science Foundation (NSF) under Award CBET-1032330.

■ REFERENCES

(1) Novoselov, K. S.; Geim, A. K.; Morozov, S. V.; Jiang, D.; Zhang, Y.; Dubonos, S. V.; Grigorieva, I. V.; Firsov, A. A. *Science* **2004**, *306*, 666.

(2) Li, D.; Muller, M. B.; Gilje, S.; Kaner, R. B.; Wallace, G. G. *Nat. Nanotechnol.* **2008**, *3*, 101.
(3) Stankovich, S.; Dikin, D. A.; Dommett, G. H. B.; Kohlhaas, K. M.; Zimney, E. J.; Stach, E. A.; Piner, R. D.; Nguyen, S. T.; Ruoff, R. S. *Nature* **2006**, *442*, 282.
(4) Kim, H.; Macosko, C. W. *Macromolecules* **2008**, *41*, 3317.
(5) Kim, H.; Macosko, C. W. *Polymer* **2009**, *50*, 3797.
(6) Blake, P.; Brimicombe, P. D.; Nair, R. R.; Booth, T. J.; Jiang, D.; Schedin, F.; Ponomarenko, L. A.; Morozov, S. V.; Gleeson, H. F.; Hill, E. W.; Geim, A. K.; Novoselov, K. S. *Nano Lett.* **2008**, *8*, 1704.
(7) Li, X. L.; Zhang, G. Y.; Bai, X. D.; Sun, X. M.; Wang, X. R.; Wang, E.; Dai, H. J. *Nature Nanotechnol.* **2008**, *3*, 538.
(8) Geim, A. K.; Novoselov, K. S. *Nat. Mater.* **2007**, *6*, 183.
(9) Novoselov, K. S.; Jiang, D.; Schedin, F.; Booth, T. J.; Khotkevich, V. V.; Morozov, S. V.; Geim, A. K. *Proc. Natl. Acad. Sci. U.S.A.* **2005**, *102*, 10451.
(10) Obraztsov, A. N. *Nat. Nanotechnol.* **2009**, *4*, 212.
(11) Stankovich, S.; Dikin, D. A.; Piner, R. D.; Kohlhaas, K. A.; Kleinhammes, A.; Jia, Y.; Wu, Y.; Nguyen, S. T.; Ruoff, R. S. *Carbon* **2007**, *45*, 1558.
(12) Park, S.; An, J. H.; Jung, I. W.; Piner, R. D.; An, S. J.; Li, X. S.; Velamakanni, A.; Ruoff, R. S. *Nano Lett.* **2009**, *9*, 1593.
(13) Jung, I.; Dikin, D.; Park, S.; Cai, W.; Mielke, S. L.; Ruoff, R. S. *J. Phys. Chem. C* **2008**, *112*, 20264.
(14) Rourke, J. P.; Pandey, P. A.; Moore, J. J.; Bates, M.; Kinloch, I. A.; Young, R. J.; Wilson, N. R. *Angew. Chem., Int. Ed.* **2011**, *50*, 3173–3177.
(15) McAllister, M. J.; Li, J. L.; Adamson, D. H.; Schniepp, H. C.; Abdala, A. A.; Liu, J.; Herrera-Alonso, M.; Milius, D. L.; Car, R.; Prud'homme, R. K.; Aksay, I. A. *Chem. Mater.* **2007**, *19*, 4396.
(16) Ansari, S.; Giannelis, E. P. *J. Polym. Sci., Part B: Polym. Phys.* **2009**, *47*, 888.
(17) Schniepp, H. C.; Li, J. L.; McAllister, M. J.; Sai, H.; Herrera-Alonso, M.; Adamson, D. H.; Prud'homme, R. K.; Car, R.; Saville, D. A.; Aksay, I. A. *J. Phys. Chem. B* **2006**, *110*, 8535.
(18) Lee, Y. R.; Raghu, A. V.; Jeong, H. M.; Kim, B. K. *Macromol. Chem. Phys.* **2009**, *210*, 1247.
(19) Gomez-Navarro, C.; Weitz, R. T.; Bittner, A. M.; Scolari, M.; Mews, A.; Burghard, M.; Kern, K. *Nano Lett.* **2007**, *7*, 3499.
(20) Hernandez, Y.; Nicolosi, V.; Lotya, M.; Blighe, F. M.; Sun, Z. Y.; De, S.; McGovern, I. T.; Holland, B.; Byrne, M.; Gun'ko, Y. K.; Boland, J. J.; Niraj, P.; Duesberg, G.; Krishnamurthy, S.; Goodhue, R.; Hutchison, J.; Scardaci, V.; Ferrari, A. C.; Coleman, J. N. *Nature Nanotechnol.* **2008**, *3*, 563.
(21) Khan, U.; O'Neill, A.; Lotya, M.; De, S.; Coleman, J. N. *Small* **2010**, *6*, 864.
(22) Behabtu, N.; Lomeda, J. R.; Green, M. J.; Higginbotham, A. L.; Sinitskii, A.; Kosynkin, D. V.; Tsentalovich, D.; Parra-Vasquez, A. N. G.; Schmidt, J.; Kesselman, E.; Cohen, Y.; Talmon, Y.; Tour, J. M.; Pasquali, M. *Nature Nanotechnol.* **2010**, *5*, 406.
(23) Valles, C.; Drummond, C.; Saadaoui, H.; Furtado, C. A.; He, M.; Roubeau, O.; Ortolani, L.; Monthioux, M.; Penicaud, A. *J. Am. Chem. Soc.* **2008**, *130*, 15802.
(24) Viculis, L. M.; Mack, J. J.; Mayer, O. M.; Hahn, H. T.; Kaner, R. B. *J. Mater. Chem.* **2005**, *15*, 974.
(25) Pupysheva, O. V.; Farajian, A. A.; Knick, C. R.; Zhamu, A.; Jang, B. Z. *J. Phys. Chem. C* **2010**, *114*, 21083.
(26) Bourlinos, A. B.; Georgakilas, V.; Zboril, R.; Steriotis, T. A.; Stubos, A. K.; Trapalis, C. *Solid State Commun.* **2009**, *149*, 2172.
(27) Vadukumpully, S.; Paul, J.; Valiyaveettil, S. *Carbon* **2009**, *47*, 3288.
(28) De, S.; King, P. J.; Lotya, M.; O'Neill, A.; Doherty, E. M.; Hernandez, Y.; Duesberg, G. S.; Coleman, J. N. *Small* **2010**, *6*, 458.
(29) Green, A. A.; Hersam, M. C. *Nano Lett.* **2009**, *9*, 4031–4036.
(30) Lotya, M.; Hernandez, Y.; King, P. J.; Smith, R. J.; Nicolosi, V.; Karlsson, L. S.; Blighe, F. M.; De, S.; Wang, Z. M.; McGovern, I. T.; Duesberg, G. S.; Coleman, J. N. *J. Am. Chem. Soc.* **2009**, *131*, 3611.
(31) Lotya, M.; King, P. J.; Khan, U.; De, S.; Coleman, J. N. *ACS Nano* **2010**, *4*, 3155–3162.
(32) Hao, R.; Qian, W.; Zhang, L. H.; Hou, Y. L. *Chem. Commun.* **2008**, 6576.
(33) Grady, B. P. *Macromol. Rapid Commun.* **2010**, *31*, 247–257.
(34) Rafiee, M. A.; Lu, W.; Thomas, A. V.; Zandiatashbar, A.; Rafiee, J.; Tour, J. M.; Koratkar, N. A. *ACS Nano* **2010**, *4*, 7415.
(35) Rafiee, M. A.; Rafiee, J.; Wang, Z.; Song, H.; Yu, Z.-Z.; Koratkar, N. *ACS Nano* **2009**, *3*, 3884.
(36) Yavari, F.; Rafiee, M. A.; Rafiee, J.; Yu, Z. Z.; Koratkar, N. *ACS Appl. Mater. Interfaces* **2010**, *2*, 2738.
(37) Moniruzzaman, M.; Winey, K. I. *Macromolecules* **2006**, *39*, 5194.
(38) Blighe, F. M.; Hernandez, Y. R.; Blau, W. J.; Coleman, J. N. *Adv. Mater.* **2007**, *19*, 4443.
(39) Bryning, M. B.; Milkie, D. E.; Islam, M. F.; Kikkawa, J. M.; Yodh, A. G. *Appl. Phys. Lett.* **2005**, *87*, 3.
(40) Tung, V. C.; Chen, L. M.; Allen, M. J.; Wassei, J. K.; Nelson, K.; Kaner, R. B.; Yang, Y. *Nano Lett.* **2009**, *9*, 1949.
(41) Wu, J.; Harwell, J. H.; O'Rear, E. A. *J. Phys. Chem.* **1987**, *91*, 623.
(42) Sakhalkar, S. S.; Hirt, D. E. *Langmuir* **1995**, *11*, 3369.
(43) Pongprayoon, T.; Yanumet, N.; O'Rear, E. A. *J. Colloid Interface Sci.* **2002**, *249*, 227.
(44) Wu, J.; Harwell, J. H.; O'Rear, E. A. *Langmuir* **1987**, *3*, 531.
(45) Karlsson, P. M.; Esbjörnsson, N. B.; Holmberg, K. *J. Colloid Interface Sci.* **2009**, *337*, 364.
(46) Carswell, A. D. W.; O'Rea, E. A.; Grady, B. P. *J. Am. Chem. Soc.* **2003**, *125*, 14793.
(47) Ha, M. L. P.; Grady, B. P.; Lolli, G.; Resasco, D. E.; Ford, W. T. *Macromol. Chem. Phys.* **2007**, *208*, 446.
(48) Marquez, M.; Patel, K.; Carswell, A. D. W.; Schmidtke, D. W.; Grady, B. P. *Langmuir* **2006**, *22*, 8010.
(49) Marquez, M.; Kim, S.; Jung, J.; Truong, N.; Teeters, D.; Grady, B. P. *Langmuir* **2007**, *23*, 10008.
(50) Yuan, W.-L.; O'Rear, E. A.; Grady, B. P.; Glatzhofer, D. T. *Langmuir* **2002**, *18*, 3343.
(51) Wang, R. K.; Chen, W. C.; Campos, D. K.; Ziegler, K. J. *J. Am. Chem. Soc.* **2008**, *130*, 16330.
(52) Chen, W. C.; Wang, R. K.; Ziegler, K. J. *ACS Appl. Mater. Interfaces* **2009**, *1*, 1821.
(53) Hait, S. K.; Majhi, P. R.; Blume, A.; Moulik, S. P. *J. Phys. Chem. B* **2003**, *107*, 3650.
(54) Rai, P. K.; Pinnick, R. A.; Parra-Vasquez, A. N. G.; Davis, V. A.; Schmidt, H. K.; Hauge, R. H.; Smalley, R. E.; Pasquali, M. *J. Am. Chem. Soc.* **2006**, *128*, 591.
(55) Ferrari, A. C.; Meyer, J. C.; Scardaci, V.; Casiraghi, C.; Lazzeri, M.; Mauri, F.; Piscanec, S.; Jiang, D.; Novoselov, K. S.; Roth, S.; Geim, A. K. *Phys. Rev. Lett.* **2006**, *97*, 4.
(56) Asnachinda, E.; O'Haver, J. H.; Sabatini, D. A.; Khaodhiar, S. *J. Appl. Polym. Sci.* **2010**, *115*, 1145.
(57) See, C. H.; O'Haver, J. H. *Colloids Surf., A* **2004**, *243*, 169.
(58) Ren, L. L.; Liu, T. X.; Guo, J. A.; Guo, S. Z.; Wang, X. Y.; Wang, W. Z. *Nanotechnology* **2010**, *21*, 7.
(59) Duque, J. G.; Cognet, L.; Parra-Vasquez, A. N. G.; Nicholas, N.; Schmidt, H. K.; Pasquali, M. *J. Am. Chem. Soc.* **2008**, *130*, 2626.